Polyisoprene Captured Sulfur Nanocomposite Materials for High Areal Capacity Lithium Sulfur Battery

Zeheng Li,§ Chen Fang†, Chao Qian,§ Shudong Zhou§, Xiangyun Song†, Min. Ling§ Chengdu Liang§, Gao Liu†**

§ Key Laboratory of Biomass Chemical Engineering of Ministry of Education, College of Chemical and Biological Engineering, Zhejiang University, Hangzhou 310027, China.

† Energy Storage and Distributed Resources Division, Lawrence Berkeley National Laboratory, Berkeley, California 94720, United States.

KEYWORDS: polyisoprene, inverse vulcanization, binder, shuttle effects, lithium sulfur battery

ABSTRACT: A polyisoprene-sulfur (PIPS) copolymer and nano sulfur composite materials (90 wt% sulfur) is synthesized through inverse vulcanization of PIP polymer with sulfur micron size particles for high areal capacity lithium sulfur batteries. The polycrystalline structure and nanodomain nature of the copolymer are revealed through high-resolution transmission electron microscopy (HRTEM). PIP polymer is also used as binders for the electrode to further capture the dissovlved polysulfides. A high areal capacity of ca. 7.0 mAh/cm^2 and stable cycling are achieved

based on the PIPS nanosulfur composite with a PIP binder, crucial to commercialization of lithium sulfur batteries. The chemical confinement both at material and electrode level alleviates the diffusion of polysulfides and the shuttle effect. The sulfur electrodes, both fresh and cycled, are analyzed through the scanning electron microscopy (SEM). This approach enables scalable materials production and high sulfur utilization in the cell level.

1. INTRODUCTION

Due to sulfur's high theoretical capacity, nature abundance and low material cost, lithium sulfur (Li-S) cells are the ideal choice for the next-generation energy storage devices for emerging technologies, e.g., unmanned aerial vehicles (UAV) and air-taxi, and short-duration electric airplane. However, sulfur is an electronic insulator with a conductivity of ca. 1×10^{-16} S m^{-1} at 20 °C, leading to low sulfur utilization and limited rate capabilities. Another critical issue is the 'shuttle effect'. The elemental sulfur is not reduced directly to the final products, as low-order polysufides (Li_2S_2 and Li_2S) when lithiation, instead, a multiphase process is inevitable involving the high-order polysulfide intermediates, Li_2S_n, which are soluble in electrolytes and undergo a multiple conversion steps to form many intermediate states and final product. The soluble polysulfides can diffuse across the cell, invoking the polysulfide shuttle effects. Besides this effect, the volume expansion from sulfur (2.07 g cm^{-3}) to Li_2S (1.66 g cm^{-3}) is approximately 80 vol% after full lithiation.[1-6] These issues have hindered the successful development of Li-S batteries.[7-10] To solve these problems, the efforts on Li-S batteries have mainly focused on the following aspects: carbon/sulfur composite,[11-13] metal oxide/sulfur composite[14-16] and polymer/sulfur composite.[17-25] Among these, carbon/sulfur composites are most extensively explored. Recently, metal oxide and

the metal sulfide have also gained the attention of the community due to their strong polysulfide adsorption capabilities.[26-28] In contrast, polymer/sulfur composites are both mechanically flexible and versatile in applications due to their functionality and good solubilities. The functional groups on the polymers can act as anchoring point to immobilized sulfur species to the polymer chains. The earliest reported polymer grafted polysulfide is based on a low temperature sintered polyacrylonitrile (PAN) polymer and elemental sulfur.[29] It is believed the short sulfur chains are bonded with the highly conjugated carbon nitrogen system to provide high capacity and high stabilities. A series of approaches had been explored and reported since, with many based-on encapsulation or nanocomposite hybridization of elemental sulfur by conjugated polymers to both confine polysulfide and improve electronic conductivities, e.g., polyaniline, polypyrrole and polythiophene.[30] Simple grafting of the polymer sulfide on a functional polymer either ex situ or in situ have also reported and shown improved performance.[31-37] However, combination of one polymer both as sulfur host and as binder for electrode application has never been explored.

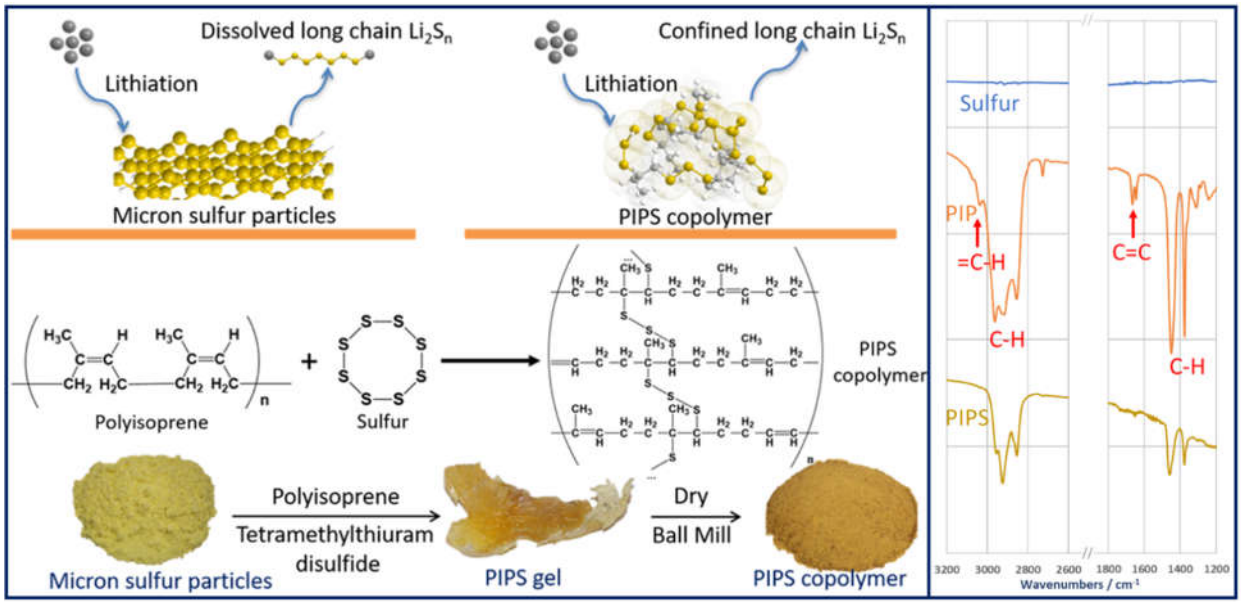

Figure 1. Left section. Long chain polysulfides confinement mechanism is illustrated at the upper part: the C-S bonds generated after vulcanization provide a reservoir for long chain polysulfides so that the polysulfides would not directly diffuse into electrolyte. The chemical transformation and material processing for PIPS preparation are shown at the lower part: polysulfides are immobilized in the polymer network. Right section. FT-IR spectra of starting materials sulfur (blue) and PIP (orange), and product PIPS (yellow).

Herein, we demonstrate a copolymer based on grafted sulfur on polyisoprene (PIP) as the electroactive materials to realize high areal capacity sulfur electrodes in Li-S batteries, and the same PIP polymers is used as electrode binders to further capture the dissolved polysulfide and provide additional stability. A toluene solution-based copolymerization is chosen to avoid evolution of gaseous byproducts (e.g., H_2S and other volatile sulfur rich molecules).[5] Meanwhile, vulcanization catalysts, i.e., tetramethylthiuram disulfide and zinc oxide, were added to promote the polysulfide addition to the polymer to form the sulfur and PIP copolymer (vulcanization) without overheating the reaction. To optimize vulcanization conditions, the effects of temperature, amount of catalyst, reaction time and feed ratios of sulfur and PIP were all explored. The copolymerization enables high sulfur content polyisoprene-sulfur (PIPS) copolymer and confined nano-sulfur phases (90 wt% sulfur) as shown in Figure 1. The confinement mechanism of dissolved polysulfides is also illustrated in Figure 1. After copolymerization, the C-S bonds can trap the long chain Li_2S_n to avoid further shuttle effect, which is also beneficial to overcome the volume expansion.[38]

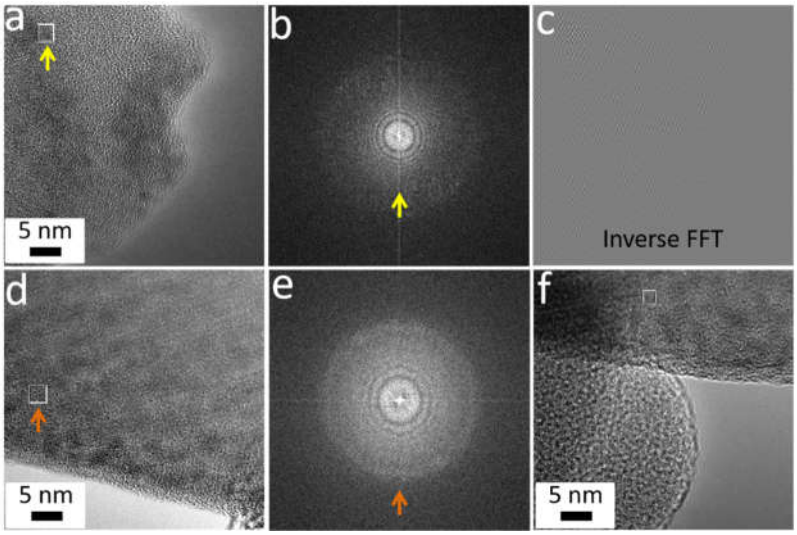

Figure 2. TEM images of the PIPS and sulfur nanocomposite materials. The polycrystalline structure is verified by the Debye rings in 1b and 1e, corresponding to the square area pointed by the arrow in 1a and 1d, respectively. 1c is the inverse fast Fourier transform (FFT) of the square area pointed in 1f.

2. RESULTS AND DISCUSSION

The synthesized PIPS was examined with FT-IR. As shown in Figure 1 (right section), the FT-IR spectrum of the starting material PIP shows a peak at 3036 cm^{-1}, indicating presence of =C-H bonds; correspondingly, the peaks at 1665 and 1643 cm^{-1} are observed for the C=C bonds. Disappearance of these peaks from the IR spectrum of PIPS demonstrates successful transformation from PIP to PIPS. The PIPS spectrum still presents very similar alkane C-H peaks as those of PIP, excluding the possibility of material decomposition.

To evaluate the properties of PIPS and sulfur nanocomposite materials, high-resolution transmission electron microscopy (HRTEM) images are collected as shown in Figure 2. Here, a typical polycrystalline structure, Debye rings in Figure 2b and 2e, is presented through inverse fast

Fourier transform (FFT). The Debye rings originated from Figure 2a and d clearly demonstrated the success of copolymerization and the incorporation of nano domain sulfur in connection with the sulfur crosslinkers. The homogeneous distribution at nano-scale is verified by the randomly distributed polycrystalline without preferred orientation. At the micro-scale, the morphology is recorded through scanning electron microscopy (SEM) as shown in Figure 3. The size of sulfur particles used for our controlled cells range from several microns to tens of microns. The dried PIPS copolymer material after ball mill is around the same particle size distribution as the sulfur precursors in Figure 3a-c. The electrochemical stability of PIP was tested using cyclic voltammetry (CV), as shown in Figure S1, which demonstrates that the PIS is inactive between 1.7 and 2.8 V. The binder coats the surface of the sulfur composite and may impede the lithium ion diffusion. Hence, the wettability of the binder is also evaluated as demonstrated in Figure S2. The total electrolyte uptake is about 22% of the final swelling weight. This number is similar to the traditional polyvinylidene fluoride binder. Afterwards, thermalgravimetric analysis (TGA) ramping to 600 °C in nitrogen at the rate of 5 °C/min is conducted as shown in Figure S2. The TGA profiles of PIPS and sulfur nanocomposite materials reveal that 30 wt% residues remain at 600 °C, which implies better thermal stability. The better thermal stability of the copolymer is a necessary condition for battery operation.

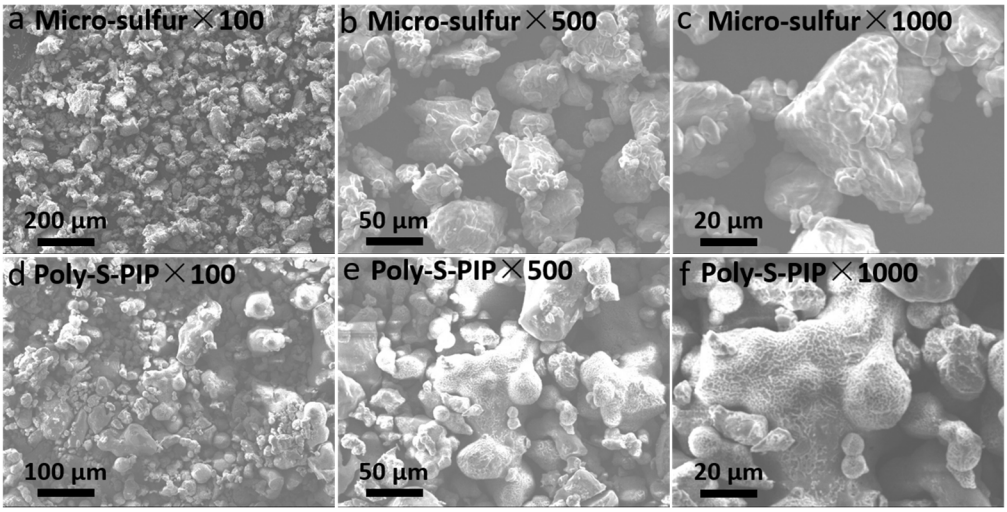

Figure 3. SEM images of (a, b, c) commercially available micron sulfur and (d, e, f) vulcanized PIPS and sulfur nanocomposite materials particles. The particle sizes of the samples vary from several microns to tens of microns. The PIPS and sulfur nanocomposite materials particles show evident network structure on the surface.

High areal capacity is critical when considering practical application. A high sulfur loading is necessary for reaching a high areal capacity.[39-43] The sulfur loading (7.0 mg_{sulfur}/cm^2) in this study is approximately 5-10 times higher than in most other nanostructured carbon-sulfur electrodes published recently (0.7-1.5 mg_{sulfur}/cm^2). The battery performance is studied in two-electrode coin cells with lithium metal as the counter electrode. Figure 4a and b portray the galvanostatic cycling performance, in terms of gravimetric and areal capacity, as a function of sulfur loading. The areal delithiation capacity of PIPS and sulfur nanocomposite materials based electrode remains above 6.5 mAh/cm^2 for ca. 30 cycles. The reason for the limited cycles is due to the dendrite growth in the lithium metal side. In regard to the lithium sulfur battery, the long cycling performance is deeply disrupted by the anode side, i.e., lithium metal, especially at such a high sulfur mass loading. As show in Figure 5, the rough dendrite appeared after even 30 cycles cycling. The

dendrites were zoomed in through SEM as presented in Figure 5d. In addition to the high areal capacity, the initial lithiation specific capacity reaches 1262 mAh/g, and is stabilized at 850 mAh/g on cycling at such a high loading. It is worth to note that a polysulfide reactive binder also play an important role to stabilized the thick sulfur electrodes during the cell operation. Polyisoprene can also directly react with the dissolved polysulfides to form a grafted polysulfide chain on the PIP polymers to further retain and confine polysulfide as shown in Figure 2a. When the polyisoprene binder is replaced by PVDF, the capacity retention decreases even for PIPS and sulfur nanocomposite materials based electrodes. The Coulombic efficiency for all PIP based electrodes is above 95%. However, the PVDF binder and elemental sulfur control electrode has much lower CE. The low CE of the controlled cells is due to the large amount of dissolution of reduced polysulfide species, which oxidized during the following delithiation process. The higher CE of PIPS based electrode proves the effective control of polysulfide diffusion of PIPS and sulfur nanocomposite materials based electrode.[44] Panels d, e, f show typical lithiation/delithition profiles of the elemental sulfur and PIPS and sulfur nanocomposite materials based electrodes. The lithiation profile show two plateaus at around 2.3 and 2.1 V versus Li/Li^+. The plateau at ca. 2.3 V is corresponded to the reduction of sulfur to higher-order lithium polysufides. The plateau at ca. 2.1 V is corresponded to the transformation of higher order lithium polysulfides to low-order lithium polysulfides. The reverse reactions are indicated by two plateaus in the delithiation curves. To analyze the voltage curves in depth, the factor of delithiation-shuttle is examined as demonstrated in the following equation[4]:

$$k_s q_H [S_{total}]/I_C = f_C \qquad \text{eq. 1}$$

The parameters involved in this equation are as follows: $q_{H,}$ the specific capacity of sulfur at high plateau; k_s, shuttle constant; I_C, delithiation current; $[S_{total}]$, total concentration of sulfur; f_C,

delithiation-shuttle factor. When I_C is high enough or k_s is low enough, the value of f_C would be smaller than 1. In such a scenario, a sharp increase in voltage would be observed, which indicates complete delithiation of the cell. In Figure 4d and e, significant and sharp increases on the voltage profiles were observed for PIPS based sulfur electrodes, which serves as proof that the f_C values are < 1. The delithiation current I_C was set to be a small number, i.e., 0.05 C, and therefore, the value of shuttle constant k_s must be sufficiently small as well to make $f_C < 1$. In contrast, when $f_C > 1$, the cell would not reach a complete level of delithiation. The micron sulfur electrodes with PVDF binders only delivered higher charge plateau. This is indicator that the charging process only involved longer polysulfide species and partially lithiation/delithiation.

$$Q_{HD}=Q_{Hacc}ln(1+f_D)/f_D \quad \text{eq. 2}$$

For eq. 2, which describes lithiation curve at high plateau, the parameters are as follows: Q_{HD}, experimental lithiation capacity; Q_{Hacc}, accumulated capacity; f_D, sulfur lithiation shuttle factor. During the lithiation process, electrochemical reduction of sulfur occurs first as a result of the lithiation current, and then the reduction of long chain polysulfides on the lithium metal side starts due to the polysulfides shuttling.

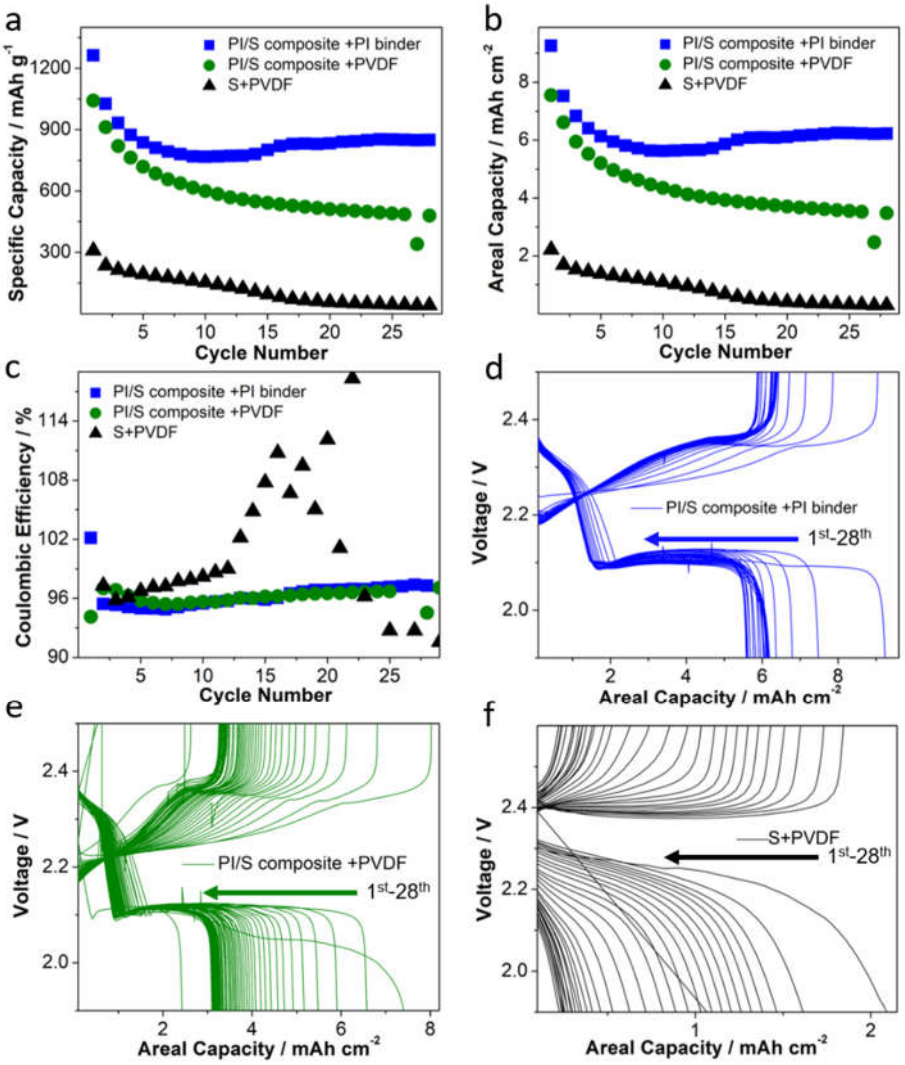

Figure 4. Electrochemical characterization of PIPS and sulfur nanocomposite materials based sulfur electrode and comparison to micron sulfur based electrode. The composition of cathode is PIPS and sulfur nanocomposite materials:C45:Graphene:binder=6:2:1:1 (weight ratio). The sulfur content in PIPS and sulfur nanocomposite materials is 90 wt%. a, b ,c, Cycling stability comparison of PIPS and sulfur nanocomposite materials based sulfur electrode versus micron sulfur based electrode at around 0.47 mA/cm^2 at 30 °C. d, e, f galvanostatic lithiation and delithiation.

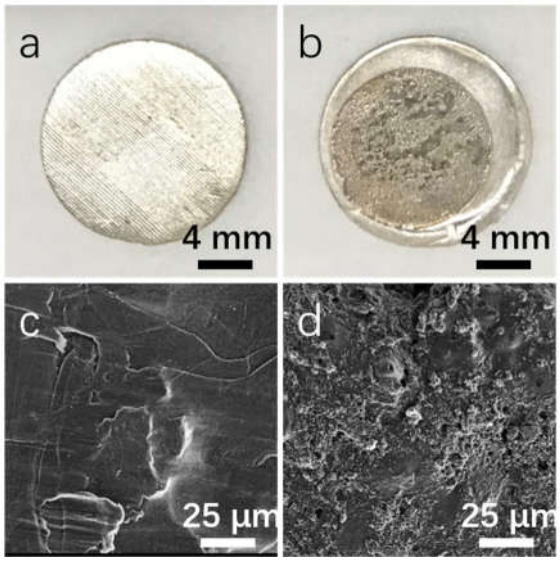

Figure 5. The morphology of dendrite growth after 30 cycles. a, c, optical and SEM images of the pristine lithium metal; b, d, optical and SEM images of the dendrite after dioxolane washing.

Based on the eq. 2, the value of Q_{HD} could reach that of Q_{Hacc} only when the value of f_D is close to zero. The f_D value could approach zero with a lithiation current that is sufficiently high or with a shuttle constant that is sufficiently low. In this work, the PIPS and sulfur nanocomposite materials based electrodes were lithiated with a rather small current, i.e., 0.04C (Figure 4d and e). Therefore, a well-controlled, namely very low shuttle constant must have been delivered by the PIPS/sulfur cells, which is a significant improvement comparing to lithiation profiles of PVDF/sulfur cells (see Figure 4f). The copolymerized PIPS and sulfur nanocomposite materials clearly performs very well as a sulfur confinement mediate even under rigorous conditions (7 mg_{sulfur}/cm^2, C/25) as shown in Figure 4.

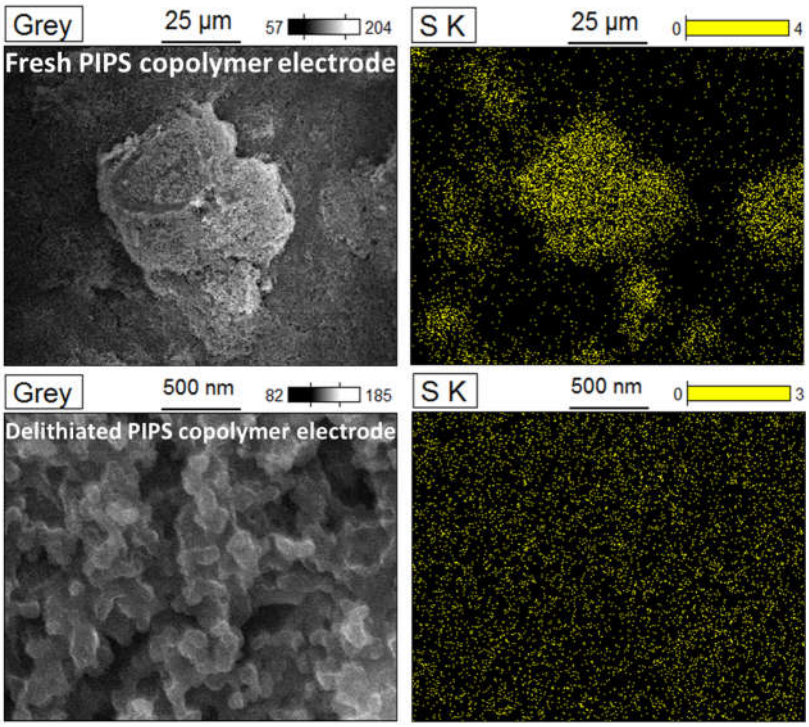

Figure 6. SEM images of Poly-S-PIP based sulfur electrodes and its Energy Dispersive Spectra (EDS) mapping.

All fresh prepared cathodes show a micron sulfur grains on the electrode surface, which can be proved in the Energy Dispersive Spectra (EDS) mapping in Figure 6. To track the morphology evolution after lithiation/delithiation, SEM images of PIPS and sulfur nanocomposite materials based electrodes are collected as shown in Figure 7. In fully delithiated state, the micron sulfur particles disappear totally. The sulfur element is detected after zoom into nano-scale, which means the better dispersion of sulfur in the cathode matrix after delithiation. In contrast, the micron sulfur based electrode still shows bulk sulfur particles after lithiation/delithiation. The existing bulk particles indicate that the sulfur is not fully utilized. The reveal of the morphology is in accord with the electrochemical performance of cathode.

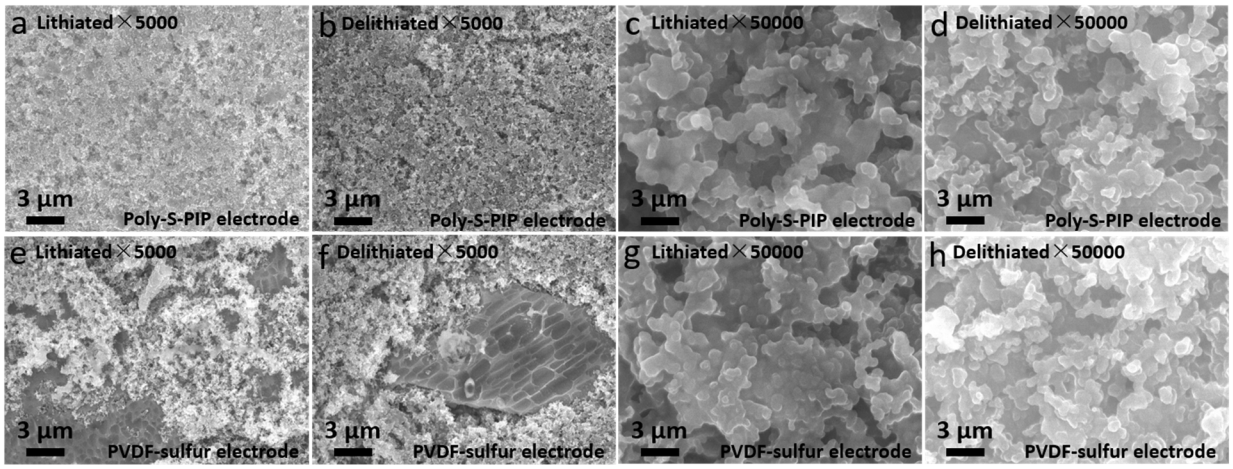

Figure 7. SEM images of the lithiated/delithiated electrodes based on PIPS copolymer (a, b, c, d) and commercially available micron sulfur (e, f, g, h) at vary magnification.

3. CONCLUSIONS

In summary, the electrochemical lithiation process of vulcanized polyisoprenes that contain covalently immobilized sulfur chains were examined, and a significant performance enhancement was observed by comparing the results to those of the isolated elemental sulfur particles. The lithiation/delithiation shuttle factor is proved to be low enough even at a very small lithiation/delithiation currrent. The vulcanized strategy presents a promising areal capacity of 6.5 mAh/cm^2 during cycling. We also expect that further optimization of the copolymers structure can lead to better performance of the polymer based sulfur electrode system.

ASSOCIATED CONTENT

Supporting Information.

The Supporting Information is available free of charge on the ACS Publications website at DOI: 10. 1021 / acaami. 8bxxxxx.

Detailed description of the experiments; additional figure about TGA characterization of micron sulfur and PIPS and sulfur nanocomposite materials.

AUTHOR INFORMATION

Corresponding Author

***E-mail: gliu@lbl.gov (G.L.).**

***E-mail: minling@zju.edu.cn (M.L.).**

Notes

The authors declare no competing financial interest.

ACKNOWLEDGMENT

This work is funded by the Assistant Secretary for Energy Efficiency, Vehicle Technologies Office of the U.S. Department of Energy, under the Advanced Battery Materials Research (BMR) Program and by the Director, Office of Science, Office of Basic Energy Sciences, of the US Department of Energy under contract no. DE-AC02-05CH11231. Z.L., C.Q. and M.L. are partially supported by National Natural Science Foundation of China (21476194), 1000 Youth Talent Project, the National Key R &D Program of China (Grant No. 2018YFB0104300)

REFERENCES

(1) Bresser, D.; Passerini, S.; Scrosati, B., Recent progress and remaining challenges in sulfur-based lithium secondary batteries - a review. *Chem. Commun.* **2013**, *49*, 10545-10562.

(2) Manthiram, A.; Fu, Y. Z.; Chung, S. H.; Zu, C. X.; Su, Y. S., Rechargeable Lithium-Sulfur Batteries. *Chem. Rev.* **2014**, *114*, 11751-11787.

(3) Lin, C. N.; Chen, W. C.; Song, Y. F.; Wang, C. C.; Tsai, L. D.; Wu, N. L., Understanding dynamics of polysulfide dissolution and re-deposition in working lithium-sulfur battery by in-operando transmission X-ray microscopy. *J. Power Sources* **2014**, *263*, 98-103.

(4) Mikhaylik, Y. V.; Akridge, J. R., Polysulfide shuttle study in the Li/S battery system. *J. Electrochem. Soc.* **2004**, *151*, A1969-A1976.

(5) Ai, G.; Dai, Y.; Ye, Y.; Mao, W.; Wang, Z.; Zhao, H.; Chen, Y.; Zhu, J.; Fu, Y.; Battaglia, V.; Guo, J.; Srinivasan, V.; Liu, G., Investigation of surface effects through the application of the functional binders in lithium sulfur batteries. *Nano Energy* **2015**, *16*, 28-37.

(6) Chen, W.; Lei, T. Y.; Lv, W. Q.; Hu, Y.; Yan, Y. C.; Jiao, Y.; He, W. D.; Li, Z. H.; Yan, C. L.; Xiong, J., Atomic Interlamellar Ion Path in High Sulfur Content Lithium-Montmorillonite Host Enables High-Rate and Stable Lithium-Sulfur Battery. *Adv. Mater.* **2018**, *30*, 1804084.

(7) Yao, N. P.; Heredy, L. A.; Saunders, R. C., Secondary Lithium-Sulfur Battery. *J. Electrochem. Soc.* **1970**, *117*, C247-&.

(8) Heredy, L. A.; Parkins, W. E., Lithium-Sulfur Battery Plant for Power Peaking. *Ieee T. Power. Ap. Syst.* **1972**, *Pa91*, 1731-&.

(9) Lei, T. Y.; Chen, W.; Lv, W. Q.; Huang, J. W.; Zhu, J.; Chu, J. W.; Yan, C. Y.; Wu, C. Y.; Yan, Y. C.; He, W. D.; Xiong, J.; Li, Y. R.; Yan, C. L.; Goodenough, J. B.; Duan, X. F., Inhibiting Polysulfide Shuttling with a Graphene Composite Separator for Highly Robust Lithium-Sulfur Batteries. *Joule* **2018**, *2*, 2091-2104.

(10) Chen, W.; Lei, T. Y.; Wu, C. Y.; Deng, M.; Gong, C. H.; Hu, K.; Ma, Y. C.; Dai, L. P.; Lv, W. Q.; He, W. D.; Liu, X. J.; Xiong, J.; Yan, C. L., Designing Safe Electrolyte Systems for a High-Stability Lithium-Sulfur Battery. *Adv. Energy Mater.* 2018, 8, 1702348.

(11) Li, Z.; Huang, Y. M.; Yuan, L. X.; Hao, Z. X.; Huang, Y. H., Status and prospects in sulfur-carbon composites as cathode materials for rechargeable lithium-sulfur batteries. *Carbon* **2015**, *92*, 41-63.

(12) Mahmood, N.; Zhang, C. Z.; Yin, H.; Hou, Y. L., Graphene-based nanocomposites for energy storage and conversion in lithium batteries, supercapacitors and fuel cells. *J. Mater. Chem. A* **2014**, *2*, 15-32.

(13) Wang, D. W.; Zeng, Q. C.; Zhou, G. M.; Yin, L. C.; Li, F.; Cheng, H. M.; Gentle, I. R.; Lu, G. Q. M., Carbon-sulfur composites for Li-S batteries: status and prospects. *J. Mater. Chem. A* **2013**, *1*, 9382-9394.

(14) Liang, X.; Kwok, C. Y.; Lodi-Marzano, F.; Pang, Q.; Cuisinier, M.; Huang, H.; Hart, C. J.; Houtarde, D.; Kaup, K.; Sommer, H.; Brezesinski, T.; Janek, J.; Nazar, L. F., Tuning Transition Metal Oxide-Sulfur Interactions for Long Life Lithium Sulfur Batteries: The "Goldilocks" Principle. *Adv. Energy Mater.* **2016**, *6*, 1501636.

(15) Bao, W. Z.; Zhang, Z. A.; Qu, Y. H.; Zhou, C. K.; Wang, X. W.; Li, J., Confine sulfur in mesoporous metal-organic framework @ reduced graphene oxide for lithium sulfur battery. *J. Alloys Compd.* **2014**, *582*, 334-340.

(16) Lei, T. Y.; Xie, Y. M.; Wang, X. F.; Miao, S. Y.; Xiong, J.; Yan, C. L., TiO2 Feather Duster as Effective Polysulfides Restrictor for Enhanced Electrochemical Kinetics in Lithium-Sulfur Batteries. *Small* **2017**, *13*, 1701013.
(17) Nagata, H.; Chikusa, Y., All-solid-state Lithium-Sulfur Batteries Using a Conductive Composite Containing Activated Carbon and Electroconductive Polymers. *Chem. Lett.* **2014**, *43*, 1335-1336.
(18) Kong, W. B.; Sun, L.; Wu, Y.; Jiang, K. L.; Li, Q. Q.; Wang, J. P.; Fan, S. S., Binder-free polymer encapsulated sulfur-carbon nanotube composite cathodes for high performance lithium batteries. *Carbon* **2016**, *96*, 1053-1059.
(19) Wang, J. K.; Yue, K. Q.; Zhu, X. D.; Wang, K. L.; Duan, L. F., C-S@PANI composite with a polymer spherical network structure for high performance lithium-sulfur batteries. *Phys. Chem. Chem. Phys.* **2016**, *18*, 261-266.
(20) Duan, L.; Lu, J. C.; Liu, W. Y.; Huang, P.; Wang, W. S.; Liu, Z. C., Fabrication of conductive polymer-coated sulfur composite cathode materials based on layer-by-layer assembly for rechargeable lithium-sulfur batteries. *Colloid Surf., A* **2012**, *414*, 98-103.
(21) Wang, X. W.; Zhang, Z. A.; Yan, X. L.; Qu, Y. H.; Lai, Y. Q.; Li, J., Interface polymerization synthesis of conductive polymer/graphite oxide@sulfur composites for high-rate lithium-sulfur batteries. *Electrochim. Acta* **2015**, *155*, 54-60.
(22) Xiao, L. F.; Cao, Y. L.; Xiao, J.; Schwenzer, B.; Engelhard, M. H.; Saraf, L. V.; Nie, Z. M.; Exarhos, G. J.; Liu, J., Molecular structures of polymer/sulfur composites for lithium-sulfur batteries with long cycle life. *J. Mater. Chem. A* **2013**, *1*, 9517-9526.
(23) Liu, J.; Galpaya, D. G. D.; Yan, L.; Sun, M.; Lin, Z.; Yan, C.; Liang, C.; Zhang, S., Exploiting a robust biopolymer network binder for an ultrahigh-areal-capacity Li–S battery. *Energy Environ. Sci.* **2017**, *10*, 750-755.
(24) Chen, W.; Lei, T. Y.; Qian, T.; Lv, W. Q.; He, W. D.; Wu, C. Y.; Liu, X. J.; Liu, J.; Chen, B.; Yan, C. L.; Xiong, J., A New Hydrophilic Binder Enabling Strongly Anchoring Polysulfides for High-Performance Sulfur Electrodes in Lithium-Sulfur Battery. *Adv. Energy Mater.* **2018**, *8*, 1702889.
(25) Fu, C. Y.; Li, G. H.; Zhang, J.; Cornejo, B.; Piao, S. S.; Bozhilov, K. N.; Haddon, R. C.; Guo, J. C., Electrochemical Lithiation of Covalently Bonded Sulfur in Vulcanized Polyisoprene. *Acs Energy Lett.* **2016**, *1*, 115-120.
(26) Zhou, G. M.; Tian, H. Z.; Jin, Y.; Tao, X. Y.; Liu, B. F.; Zhang, R. F.; Seh, Z. W.; Zhuo, D.; Liu, Y. Y.; Sun, J.; Zhao, J.; Zu, C. X.; Wu, D. S.; Zhang, Q. F.; Cui, Y., Catalytic oxidation of Li2S on the surface of metal sulfides for Li-S batteries. *Proc. Nat. Acad. Sci. U.S.A.* **2017**, *114*, 840-845.
(27) Tao, X. Y.; Wang, J. G.; Liu, C.; Wang, H. T.; Yao, H. B.; Zheng, G. Y.; Seh, Z. W.; Cai, Q. X.; Li, W. Y.; Zhou, G. M.; Zu, C. X.; Cui, Y., Balancing surface adsorption and diffusion of lithium-polysulfides on nonconductive oxides for lithium-sulfur battery design. *Nat. Commun.* **2016**, *7*, 11203.
(28) Pang, Q.; Kundu, D.; Cuisinier, M.; Nazar, L. F., Surface-enhanced redox chemistry of polysulphides on a metallic and polar host for lithium-sulphur batteries. *Nat. Commun.* **2014**, *5*, 4759.
(29) Wang, J. L.; Yang, J.; Xie, J. Y.; Xu, N. X., A novel conductive polymer-sulfur composite cathode material for rechargeable lithium batteries. *Adv. Mater.* **2002**, *14*, 963-965.
(30) Cheng, H.; Wang, S. P., Recent progress in polymer/sulphur composites as cathodes for rechargeable lithium-sulphur batteries. *J. Mater. Chem. A* **2014**, *2*, 13783-13794.
(31) Griebel, J. J.; Li, G. X.; Glass, R. S.; Char, K.; Pyun, J., Kilogram Scale Inverse

Vulcanization of Elemental Sulfur to Prepare High Capacity Polymer Electrodes for Li-S Batteries. *J. Polym. Sci. Pol. Chem.* **2015**, *53*, 173-177.
(32) Zhang, Y. Y.; Griebel, J. J.; Dirlam, P. T.; Nguyen, N. A.; Glass, R. S.; Mackay, M. E.; Char, K.; Pyun, J., Inverse vulcanization of elemental sulfur and styrene for polymeric cathodes in Li-S batteries. *J. Polym. Sci. Pol. Chem.* **2017**, *55*, 107-116.
(33) Chung, W. J.; Griebel, J. J.; Kim, E. T.; Yoon, H.; Simmonds, A. G.; Ji, H. J.; Dirlam, P. T.; Glass, R. S.; Wie, J. J.; Nguyen, N. A.; Guralnick, B. W.; Park, J.; Somogyi, A.; Theato, P.; Mackay, M. E.; Sung, Y. E.; Char, K.; Pyun, J., The use of elemental sulfur as an alternative feedstock for polymeric materials. *Nat. Chem.* **2013**, *5*, 518-524.
(34) Ling, M.; Zhang, L.; Zheng, T. Y.; Feng, J.; Guo, J. H.; Mai, L. Q.; Liu, G., Nucleophilic substitution between polysulfides and binders unexpectedly stabilizing lithium sulfur battery. *Nano Energy* **2017**, *38*, 82-90.
(35) Ling, M.; Yan, W. J.; Kawase, A.; Zhao, H.; Fu, Y. B.; Battaglia, V. S.; Liu, G., Electrostatic Polysulfides Confinement to Inhibit Redox Shuttle Process in the Lithium Sulfur Batteries. *ACS Appl. Mater. Interfaces* **2017**, *9*, 31741-31745.
(36) Zhang, L.; Ling, M.; Feng, J.; Liu, G.; Guo, J. H., Effective electrostatic confinement of polysulfides in lithium/sulfur batteries by a functional binder. *Nano Energy* **2017**, *40*, 559-565.
(37) Wang, H. L.; Ling, M.; Bai, Y.; Chen, S.; Yuan, Y. X.; Liu, G.; Wu, C.; Wu, F., Cationic polymer binder inhibit shuttle effects through electrostatic confinement in lithium sulfur batteries. *J. Mater. Chem. A* **2018**, *6*, 6959-6966.
(38) Li, G.; Ling, M.; Ye, Y.; Li, Z.; Guo, J.; Yao, Y.; Zhu, J.; Lin, Z.; Zhang, S., Acacia Senegal-Inspired Bifunctional Binder for Longevity of Lithium-Sulfur Batteries. *Adv. Energy Mater.* ***2015***, *5*, 1502878.
(39) Qie, L.; Zu, C. X.; Manthiram, A., A High Energy Lithium-Sulfur Battery with Ultrahigh-Loading Lithium Polysulfide Cathode and its Failure Mechanism. *Adv. Energy Mater.* **2016**, *6*, 1502459.
(40) Peng, H. J.; Xu, W. T.; Zhu, L.; Wang, D. W.; Huang, J. Q.; Cheng, X. B.; Yuan, Z.; Wei, F.; Zhang, Q., 3D Carbonaceous Current Collectors: The Origin of Enhanced Cycling Stability for High-Sulfur-Loading Lithium-Sulfur Batteries. *Adv. Funct. Mater.* **2016**, *26*, 6351-6358.
(41) Pang, Q.; Kundu, D.; Nazar, L. F., A graphene-like metallic cathode host for long-life and high-loading lithium-sulfur batteries. *Mater. Horiz.* **2016**, *3*, 130-136.
(42) Chang, C. H.; Chung, S. H.; Manthiram, A., Effective Stabilization of a High-Loading Sulfur Cathode and a Lithium-Metal Anode in Li-S Batteries Utilizing SWCNT-Modulated Separators. *Small* **2016**, *12*, 174-179.
(43) Wang, C.; Su, K.; Wan, W.; Guo, H.; Zhou, H. H.; Chen, J. T.; Zhang, X. X.; Huang, Y. H., High sulfur loading composite wrapped by 3D nitrogen-doped graphene as a cathode material for lithium-sulfur batteries. *J. Mater. Chem. A* **2014**, *2*, 5018-5023.
(44) Schuster, J.; He, G.; Mandlmeier, B.; Yim, T.; Lee, K. T.; Bein, T.; Nazar, L. F., Spherical ordered mesoporous carbon nanoparticles with high porosity for lithium-sulfur batteries. *Angew. Chem. Int. Ed* **2012**, *51*, 3591-395.

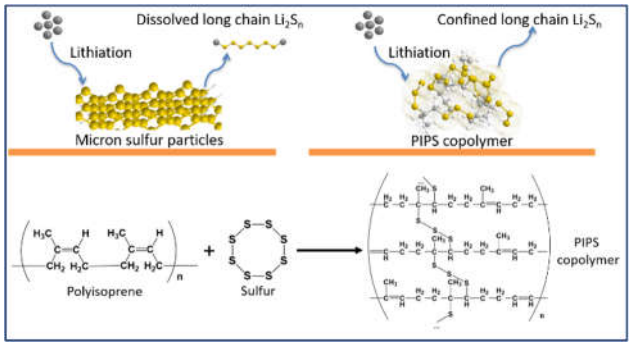

Table of Contents (TOC)